A NUMERICAL STUDY ON AERODYNAMIC RESONANCE IN TRANSONIC SEPARATED FLOW

Jens Nitzsche[1]

[1]Institute of Aeroelasticity, German Aerospace Center (DLR)
Bunsenstr. 10, 37073 Göttingen, Germany
jens.nitzsche@dlr.de

Keywords. transonic flow, stability, aerodynamic resonance, shock buffet, aileron buzz

Abstract. An ongoing numerical investigation of unsteady shock/boundary layer interaction on a 2-d supercritical airfoil in transonic flow is presented. Initially, the finite-volume URANS solver DLR-TAU is used to simulate self-sustained periodic shock oscillations well known as *shock buffet*. Next, emphasis is put on the fixed-point stability of the steady flow field below the *shock buffet onset*. Therefore the flow is perturbed in time with small sinusoidal deflections of the airfoil geometry and random impulses. With increasing angle of attack the mean flow is shown to develop a damped aerodynamic resonance, that degenerates finally towards self-amplification. The occurrence of the aerodynamic resonance is closely related to the development of shock-induced separation, accompanied by quasi-steady inverse shock motion.

1 INTRODUCTION

Beyond critical onflow conditions (in terms of Mach number Ma and angle of attack α) the transonic flow field around a fixed airfoil is known to exhibit self-sustained, large-scale shock oscillations with low frequency (typical Strouhal numbers $Sr \approx 0.1$). This phenomenon – well known as *shock buffet* – originates from the mutual interaction of the recompression shock and the boundary layer [1]. The thus induced unsteady airloads can exceed the critical limits of an aircraft's structure or become otherwise aeroelastically relevant when coupling with the structural eigenbehavior [2].

Shock buffet has been investigated experimentally for years in numerous works (e.g. [3,4]). Recent numerical studies [2,5,6] demonstrated meanwhile the ability of URANS- and DES-based CFD methods to capture the shock buffet phenomenon qualitatively. Nevertheless, the accurate prediction of the shock buffet onset, frequency and amplitude (in ascending order of complexity) remains an open challenge. This seems partly due to the limited understanding of the underlying flow physics. Although several explanations for the shock oscillations were suggested in the past (e.g. [7,8]), the actual shock buffet mechanism is still subject of discussion. Goal of the presented study is an improved understanding of the shock buffet instability, potentially leading to a more robust CFD-based modeling of the phenomenon.

An initial matter of interest is the fixed-point stability of the steady transonic flow field below the shock buffet onset, i.e. the question: How is the stable, steady flow reacting to small perturbations? In the abscence of a ready-made analytical method we choose a straightforward heuristic approach to answer the latter. Therefore we simulate the excitation of the stable, initially steady flow either by a continuing sinusoidal deflection of the airfoil geometry or by a random impulse. A time series analysis of the field response should provide some insight afterwards.
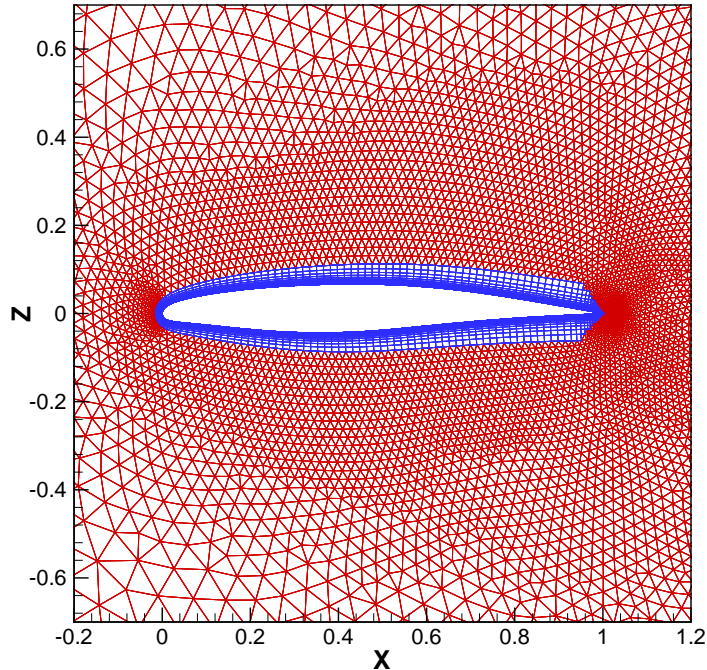
Figure 1: Detail of the unstructured grid around the supercritical airfoil BAC 3-11/RES/30/21.

2 CFD METHOD

We simulate the compressible flow around the supercritical profile BAC 3-11/RES/30/21 at $Ma = 0.75$ and Reynolds number $Re = 4.5 \times 10^6$. DLR's finite-volume based URANS solver TAU [9,10] is used on an unstructred grid with quadrilateral cells in the expected boundary layer region and triangles in the outer field. The farfield boundary is located 100 chord lengths away from the profile. For the discretization of the inviscid fluxes a central scheme with artificial scalar dissipation is applied. Since we are interested in the time-accurate dynamics of the flow, dual time stepping is used, where second-order backward differencing yields an implicit temporal discretization. The time step size is chosen case dependent between 10 and 100 steps per travelled chord length to ensure that the frequencies of interest are resolved with around 500 steps per period. Unless mentioned otherwise, turbulence closure is obtained by the 2-equation LEA k–ω model [11], which has already proven its suitability for unsteady transonic separated flows [6,12]. The widespread 1-equation model of Spalart and Allmaras [13] is occasionally used for comparison. The flow is assumed to be fully turbulent for the sake of simplicity.

3 PROCEDURES AND RESULTS

3.1 Steady behavior and shock buffet onset

For a start we compare the computed steady pressure distribution at $\alpha = 0°$ with experimental data from the cryogenic Ludwieg tube at Göttingen [14], referred to in [15]. The agreement shown in Fig. 2 is satisfactory, although the numerically predicted shock has not yet arisen to full extent in the experiment. This discrepancy is suspected to originate from wind tunnel sidewall effects not included here.

To identify the shock buffet onset for the given Mach number – i.e. the critical incidence α, where large-scale shock oscillations set in – the angle of attack is gradually changed in
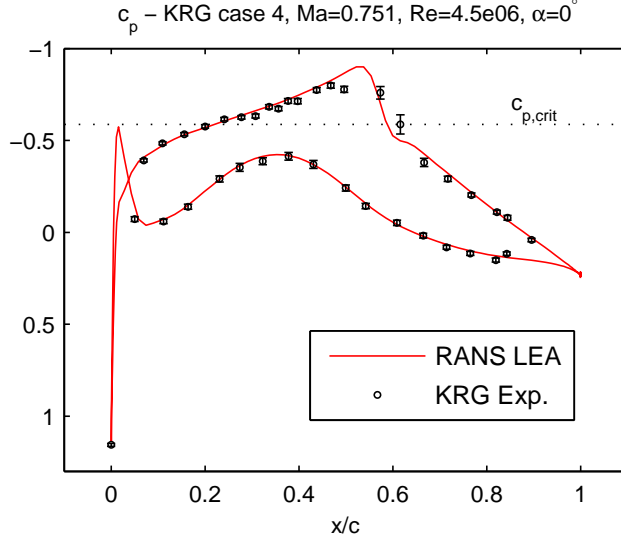
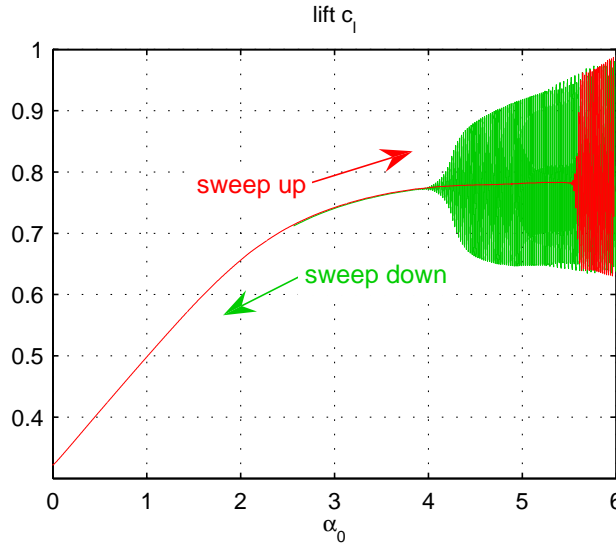Figure 2: Comparison with experimental steady flow at $\alpha = 0°$.

Figure 3: Instantaneous lift c_l during sweep runs.

time from 0° to 6° and vice versa. This linear sweep is conducted in a quasi-steady way with an angular velocity of $\pm 0.002°$ per travelled chord length.

As seen in Fig. 3, self-excited shock buffet oscillations set in catastrophically at $\alpha = 5.5°$. A limit cycle oscillation (LCO) is established with a reduced frequency[1] of $\omega^* \approx 0.62$ and a lift amplitude of ca. 20% of the mean lift. While the flow on the lower side remains subsonic and is excited passively from the trailing edge, the strong shock on the upper side oscillates self-excited with an amplitude of 23% chord by now (see Fig. 4). The boundary layer downstream of the shock separates and reattaches completely during one shock buffet cycle. The LCO amplitude grows, as α is increased further.

When reducing α back to 0° the self-excited shock oscillations persist beyond the critial α from the sweep up. Since Fig. 3 shows transient contamination (as α is not changing infinitely slow), it can only serve as an estimate to the actual LCO-amplitude-over-α

---

[1]The reduced frequency is defined in this paper with respect to farfield velocity and *full* chord as $\omega^* = \omega \cdot c / V_\infty$.
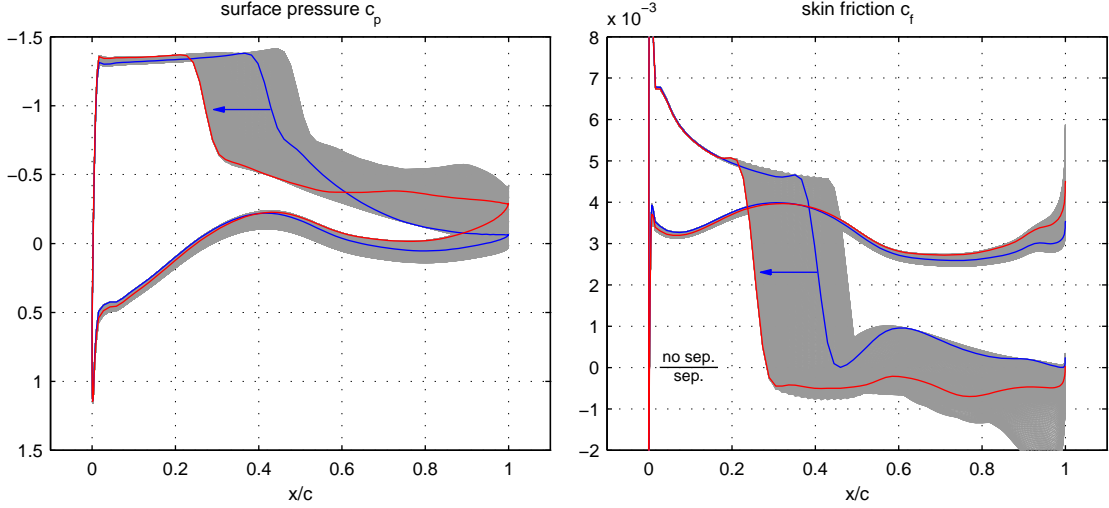
Figure 4: Ensemble of instantaneous surface pressure and skin friction distributions during one shock buffet cycle at $\alpha \approx 5.7°$. Blue and red curves show two instant states of minimal and maximal separation.
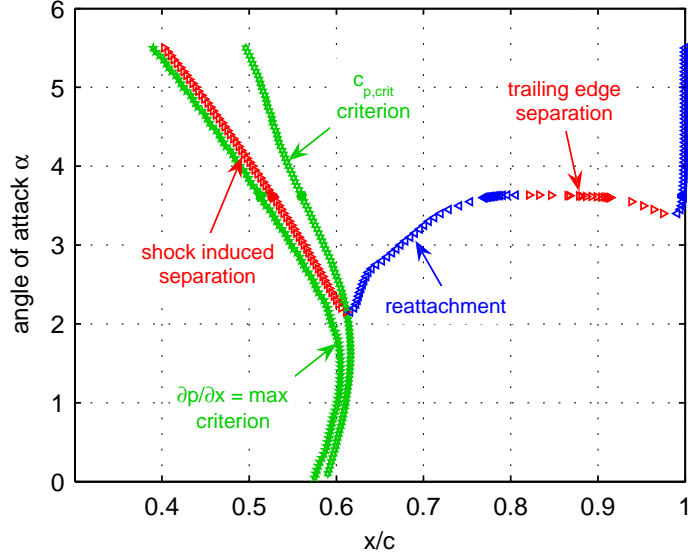

Figure 5: Location of shock foot, separation and reattachment points on the upper side during sweep up.

relation. Not shown here, unsteady computations at constant α values reveal, that a stable LCO can be observed only down to 4.5°, i.e. the oscillations shown in Fig. 3 between 4.5° and 4° are not self-sustained but damped oscillations. Nevertheless, we observe a hysteresis in the range $4.5° < \alpha < 5.5°$, which is due to the apparent coexistence of a stable shock buffet LCO alongside a stable steady flow solution (terminated by a subcritical Hopf bifurcation). Hence, the onset question cannot be answered uniquely. Straightforwardly, we define the least α, whereat shock buffet is found as the shock buffet onset. It is not yet clear, how a perturbation needs to be conditioned, to provoke a potential snap-through from the steady solution to the LCO solution.

During post-processing of the sweep response surface data we take a closer look at the instant shock foot location and possible separation and reattachment points. This is achieved by cubic spline interpolation of the surface pressure along the grid points. For identification of the shock foot position two possible criteria are tested: The shock foot is

assumed to be located, where either

1. the surface pressure intersects with the critical pressure $c_{p,crit}$ from isentropic flow relations (as plotted in Fig. 2) or
2. the surface pressure gradient $\partial c_p / \partial x$ exhibits a maximum[2].

Separation and reattachment points are identified in a similar way based on the roots of the splined skin friction distribution. The splining procedure allows virtually the resolution of shock foot and separation point displacements below the chordwise grid spacing. This will become exceedingly important in the next section, where perturbation magnitudes are kept as small as possible to avoid nonlinear effects.

Fig. 5 shows the location of those characteristic flow features on the upper side during the α increase, while the steady solution is still stable. Starting from $\alpha = 0°$ the shock moves at first downstream with increasing α, but changes direction between $1°$ and $2°$ (inverse shock motion). The upstream movement of the shock is an indicator for the increasing displacement thickness of the weakened boundary layer and is followed by the development of a separation bubble under the shock foot above $2°$. At $3.3°$ trailing edge separation sets in. Note, that backflow topology changes rapidly over a small α interval as the two separated regions merge. Above $3.8°$, we observe full shock stall. Recall, that the smallest α, where shock buffet occurs, is found at $4.5°$, i.e. fully separated flow alone is not a sufficient condition for shock buffet. Secondary, it can be seen, that the $c_{p,crit}$-criterion for the shock location diverges considerably from the maximum-gradient-criterion and the separation point as shock-/boundary layer interaction grows in strength. Hence, the latter is favored as an estimate for the actual shock position in the following.

3.2 Frequency response

In advance of the presented study it was assumed, that shock buffet is related mainly to the interplay between shock motion and the boundary layer displacement downstream of the shock. Especially, the question was raised: How is the shock reacting to small changes of the flow near the trailing edge? A mechanism, which resembles the boundary layer displacement during a shock buffet cycle is an oscillating trailing edge flap.

As the shock buffet onset is identified by now, we select four fixed-point stable flow fields at $\alpha = 0°, 2°, 3°, 4°$ whose characteristic steady or quasi-steady behaviors differ notably from each other (recall Fig. 5). These are perturbed by small deflections of a seamless 25% chord trailing edge flap. To study the sensitivity of the flow to the perturbation wave number we decide for harmonic excitation over a broad frequency range of $0.01 \leq \omega^* \leq 1$. The flap amplitude is chosen $\Delta\beta = 0.01°$. Since we change the airfoil geometry dynamically, the has to be deformed in every time step.

The imposed small deflection amplitudes cause the inherently highly nonlinear transonic flow field to behave virtually as a linear, time-invariant system. This assumption is confirmed by the observation, that following a considerable transient period after the start of an unsteady simulation all flow field variables (even in the shock region and the

---

[2]It has to be noted, that the pressure gradient maximum on the surface is always attached to the point where the oblique leg – not the normal leg — of a possible lambda shock structure impinges the surface.
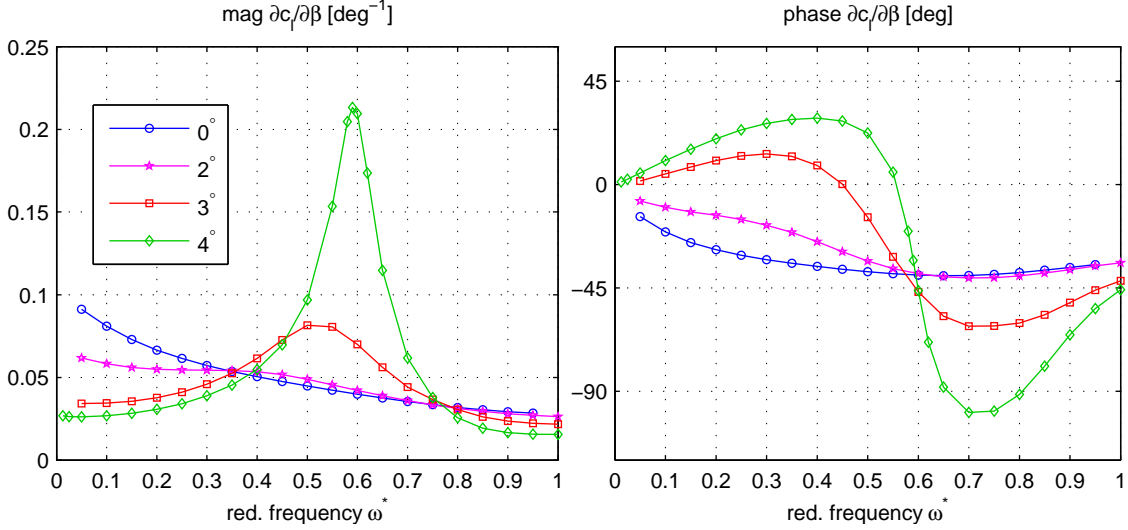
Figure 6: Frequency response of lift due to flap deflection $\partial c_l/\partial\beta$ at four different incidences.

shock displacement itself) respond almost exclusively with the excitation frequency, i.e. higher harmonics are 2-3 orders smaller than the fundamental.

Fig. 6 shows the frequency response of the complex lift derivative $\partial c_l/\partial\beta$ by means of magnitude and phase angle. Comparing the four magnitude curves, the striking difference is the complete loss of monotonicity along with the development of a pronounced resonance peak as α is increased. The resonance maximum is clearly visible for both flow fields, that feature shock-induced separation. Additionally, the 2° magnitude response has already a weak tendency towards a local maximum and one can foresee the smooth transition from the 2° curve to the 3° curve. Nevertheless, only those flow fields with separation produce an entirely unusual lift phase response: Instead of a phase lag, a phase lead can be observed starting from $\omega = 0$. This effect might serve as an indicator for the existence of shock-induced separation, if only a lift signal from a balance is available during a wind tunnel test. Passing through the resonance, phase experiences a sudden reversal, whose steepness increases along with the height of the amplitude peak. Above the phase reversal, phase drops way below the level of the fully attached flow field. Note, that not only the height of the resonance peak and the phase slope change, but also the resonance frequency itself increases slightly: At 3° the resonance is centered at $\omega^* \approx 0.53$, while at 4° it has changed to $\omega^* \approx 0.59$. It can most probably be concluded, that this resonance frequency is the very frequency of the subsequent shock buffet LCO, when α is increased further and the resonance peak is expected to approach infinity.

As the observed behaviour is very similar to a simple harmonic oscillator with one degree of freedom, we interpret the height and frequency of the resonance peak as the footprint of a conjugate complex pair of eigenvalues of an essentially linear system with the parameter α. Hence, the question for the buffet onset is most likely to be reducible to a linear stability problem, in which the critical α is found, where a complex eigenvalue crosses the imaginary axis. Recently published work from Crouch et al. [16] seems to strengthen this idea.

Since such an eigenvalue is expected to be an inherent property of the flow field alone, it should be independent of the way of excitation. To confirm the latter, we investigate
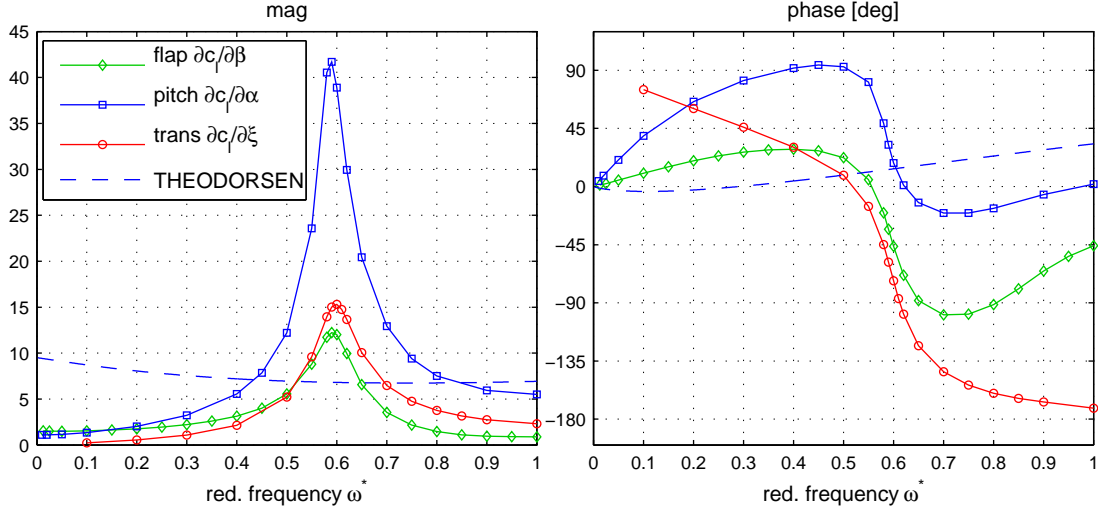
Figure 7: Frequency response of the lift derivative for different excitation kinematics at $\alpha = 4°$.

another two sinusoidal excitation kinematics besides the flap excitation, namely, pitching the whole profile around quarter-chord point with $\Delta\alpha = 0.01°$ and translating the whole profile parallel to the onflow velocity vector[3] with $\Delta\xi = 10^{-4}c$. Fig. 7 shows the resulting lift derivatives compared to those obtained by flap excitation. The resonance frequencies coincide for all of the three kinematics. Not surprisingly, pitching the whole profile has an impact on lift roughly three and a half times larger than just deflecting a flap, although in the steady limit $\omega^* \to 0$ increasing camber by flap deflection has a slightly stronger effect on lift than increasing global incidence. For the pitch excitation response we denote a resonant amplification of the unsteady airloads by a factor of ca. 40 compared to the quasi-steady lift slope at $\alpha = 4°$. For reference, Fig. 7 includes the frequency response for a flat plate pitching around quarter-chord in incompressible flow computed on the basis of classical THEODORSEN theory (scaled by $1/\sqrt{1 - Ma^2}$). The lift derivative due to translation drops to zero in the steady limit $\omega^* \to 0$, since the translational velocity $\dot{\xi}$ vanishes. Nevertheless, its phase approaches $+90°$, which indicates that in the steady case $\partial c_l / \partial \dot{\xi} > 0$ or $\partial c_l / \partial Ma < 0$ respectively.

An interesting aspect of the shock buffet resonance emerges, when we compare the complex surface pressure distributions at $\alpha = 4°$ obtained from the three different excitation kinematics outside and exactly inside the resonance. Fig. 8 shows the phase response of the surface pressure derivatives due to the three different excitations. Far below the resonance at $\omega^* = 0.2$ they differ considerably, as expected. In the resonance $\omega^* = 0.59$ they become almost congruent. The same holds of course for the magnitude not plotted here. Obviously, all of the three kinematics do now optimally excite the *shock buffet mode*, which in return dominates the overall flow field dynamics. As is known from modal testing in structural dynamics, each of the three responses in the resonance can be interpreted as a good approximation for the aerodynamic eigenvector (or "mode shape").

To stress the strangeness of the separated flow field at $\alpha = 4°$ a little more from an aeroelastic point of view, we take a closer look at certain integrals of the unsteady airloads in the sense of generalized aerodynamic forces, i.e.

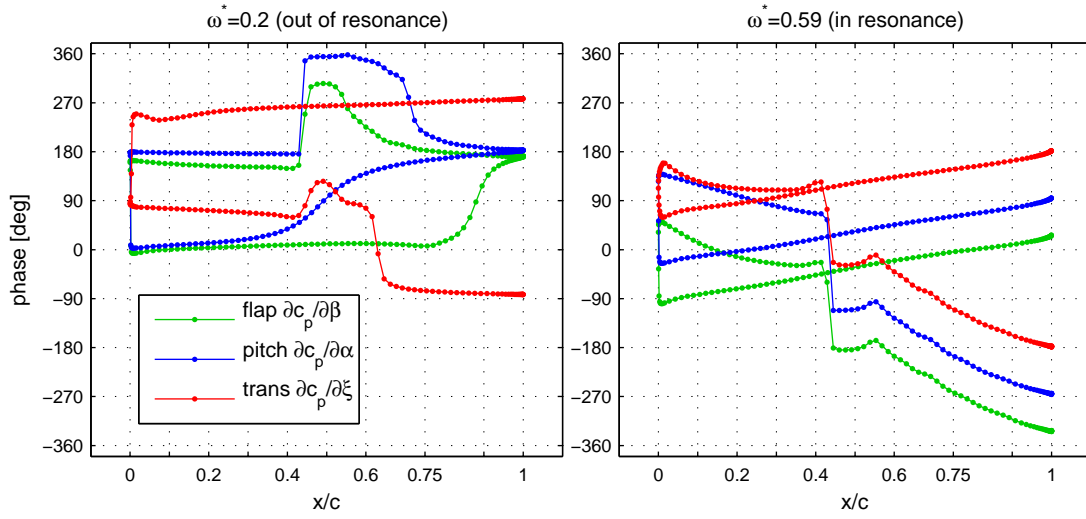[3]The translatory degree of freedom ξ is defined here positive downstream.

Figure 8: Phase response of surface pressure c_p after excitation of the $\alpha = 4°$ flow field by three different kinematics outside and inside the shock buffet response.
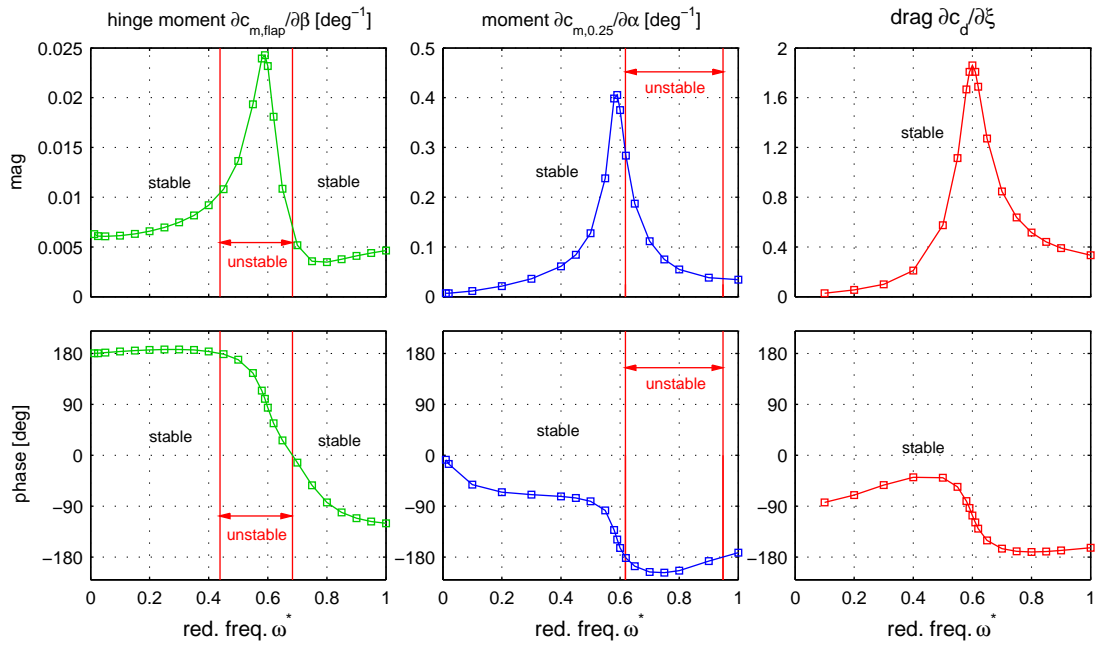

Figure 9: Generalized aerodynamic forces due to flap motion, pitching and horizontal translation at $\alpha = 4°$.
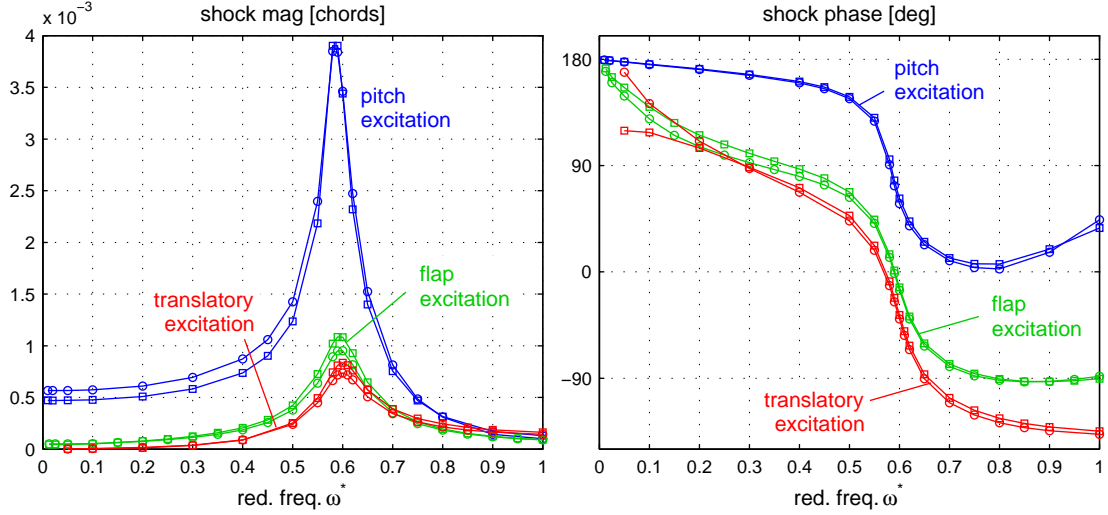
8

Figure 10: Displacement magnitude and phase with respect to excitation of the estimated shock foot (squares) and the separation point (circles) for three different excitation kinematics at $\alpha = 4°$.

1. the flap hinge moment $c_{m,flap}$ due to the flap excitation
2. the moment at quarter-chord point $c_{m,0.25}$ due to the pitch excitation and
3. the drag c_d due to the translatory excitation.

Fig. 9 shows magnitude and phase of these derivatives. Note, that when the phase of the generalized aerodynamic force becomes positive, in principle one-degree-of-freedom flutter is possible (marked as "unstable"). This effect is striking for the oscillatory flap motion, which is almost undamped for a broad frequency range starting from $\omega^* \to 0$ and for $\omega^* \gtrsim 0.43$ finally gets amplified aerodynamically by enormous airloads due to the shock buffet resonance. The latter is supposed to play an essential role in the feared "aileron buzz" phenomenon. Pure pitch motion is getting aerodynamically unstable as well for $\omega^* \gtrsim 0.63$. The translatory motion investigated here, is always stable.

To gain more insight into the observed resonance behavior, we analyze the frequency response of shock foot and separation point displacement, applying the splining method described in the previous section. Once more we select the $\alpha = 4°$ flow field and compare different excitations. Fig. 10 shows the results. Expectedly, the shock displacement amplitude exhibits a maximum in the shock buffet resonance as well. This time magnitude is not plotted as a derivative but as an absolute value in chord lengths, i.e. for the pitch excitation with $\Delta\alpha = 0.01°$ the shock foot oscillates on the surface around its mean value with a maximum amplitude of 0.4% chord and with 0.1% chord for the $\Delta\beta = 0.01°$ flap excitation. Except small deviations the separation point stays globally in phase with the shock. The phase graphs for both the flap and pitch excitation start with a phase lead of $+180°$, which indicates, that in the quasi-steady limit inverse shock motion occurs (cf. Fig. 5). The phase of the shock motion due to translation is supposed to meet $\omega^* = 0$ at $+90°$, as the shock is expected to move downstream when the onflow velocity is reduced. Nevertheless, the results in this region seem a little dubious, particularly with regard to the diverging separation point phase response. This might be due to an artefact, since during the numerical experiments the translatatory displacement amplitude $\Delta\xi$ was kept fixed instead of $\Delta\dot{\xi}$, i.e. for $\omega^* \to 0$ all unsteady signals vanish or might have become spoiled numerically.
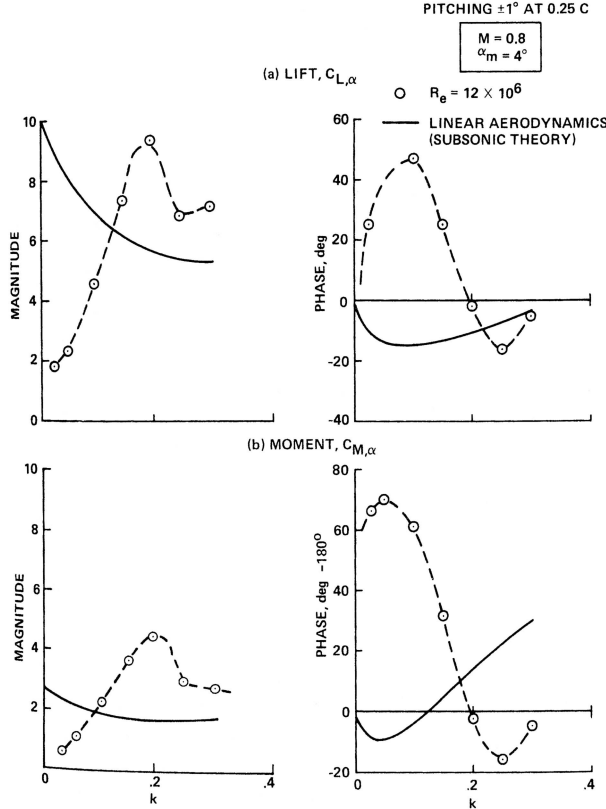
Figure 11: Frequency response of lift and moment derivatives obtained experimentally by Davis and Malcolm for a pitching NACA64A010; taken from [17]. ($\omega^* = 2k$)

In the vicinity of the resonance all of the three shock phase responses look congruent, i.e. a phase reversal of $-180°$ occurs with a characteristic slope. This refers once more to the independence of the shock buffet mode from the way of excitation. The origin of the additional $-90°$ offset in the flap and translatory excitation shock phase introduced below the resonance is not yet understood. Note, that the flap excites the flow only downstream of the shock, while the pitching and the translation excite both upstream and downstream of the shock. No explanation can be offered for the pitch shock phase behavior above $\omega^* > 0.8$, whose evolution might indicate the dominance of higher aerodynamic modes in that regime.

Emphasizing on the pitch phase response in Fig. 10, a fundamental relation can be drawn: The shock buffet eigenfrequency is located, where the shock motion of a harmonically pitching profile changes from inverse to regular shock motion. Hence, the question "Why is the shock naturally oscillating with a distinct frequency?" is augmented by another question: "Why is the shock phase reversal occuring at a distinct frequency?".

Searching through literature for experimental evidence for the undercritical resonance behavior observed in the presented CFD simulations lead finally to success in the early 1980s. Davis and Malcolm [17] noticed an unnatural (i.e. inverse) shock wave movement during shock stall on a pitching NACA64A010 at $Ma = 0.8$ and that beyond a certain frequency ($\omega^* \approx 0.3$) the real part of c_p on the upper side suddenly changes shape and resembles inviscid flow again. No adequate numerical method was available during that time to reproduce the experimental data. The most prominent result of their work is shown in Fig. 11. Note the resonance peak in both lift and moment derivative and
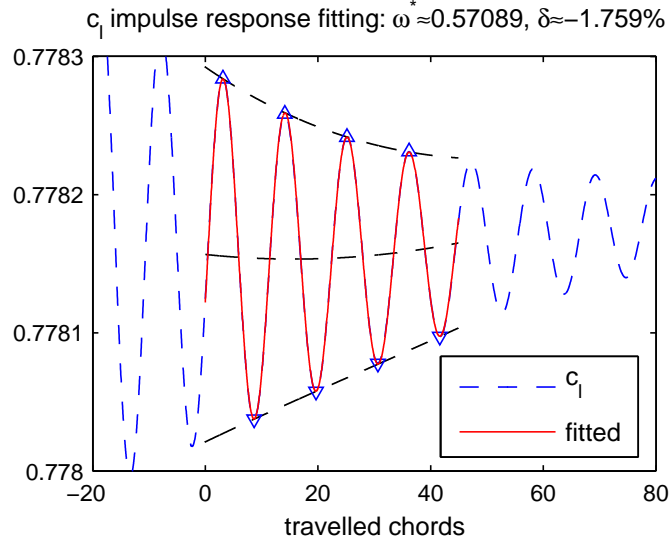
Figure 12: Part of a typical impulse response of lift c_l and fitted model curve quantifying frequency and amplification rate.

especially the phase lead of lift with respect to pitch angle below the resonance (recall Fig. 6). The positive phase of $\partial c_{m,0.25}/\partial\alpha$ (recall Fig. 9) leading to a possible one-degree-of-freedom instability was measured in the experiment as well. Houwink [18] found the same resonance behavior in forced motion experiments at $Ma = 0.75$ on a NLR7301 equipped with an oscillating trailing edge flap. The resonance frequency was measured at $\omega^* \approx 0.45$. Later indications for the shock buffet resonance can be found in [19, 20]. None of these works draws explicitly the connection from the subcritical aerodynamic resonance to self-amplified shock buffet.

3.3 Impulse response

In the preceding section it was suggested to approach the shock buffet problem in a linearized manner, i.e. we have to understand the correlation between the steady flow field and the real and imaginary part of the complex eigenvalue, that is dominating the field's global stability and unsteady behavior. Since Mach number is fixed at $Ma = 0.75$ throughout this study, the primary flow field parameter is the angle of attack α. A plain way to investigate the relation between α and the shock buffet eigenvalue is analyzing the impulse response of the flow field in time. Hence, we perturb various stable flow fields below the shock buffet onset with an impulse, whereas the numerical residual of a not so well converged steady solution serves as a random perturbation on the initial conditions of the unsteady computation. Afterwards, the transient lift response back to steady state is inspected regarding a possible oscillatory nature. If that is the case, a simple model of the form

$$c_l(t) = p(t) + \tilde{c}_l e^{\lambda t}$$

is fitted window-averaged to the lift response (cf. Fig. 12). Therein the imaginary and real part of $\lambda = \delta + i\omega^*$ contain a frequency information and an amplification rate, while the polynomial $p(t)$ captures the mean lift offset and low-frequency drifts possibly originating from unsuppressed farfield reflections. To avoid nonlinear amplitude effects only those parts of the lift response are considered, whose oscillation amplitudes fall below 0.1% of the mean value.
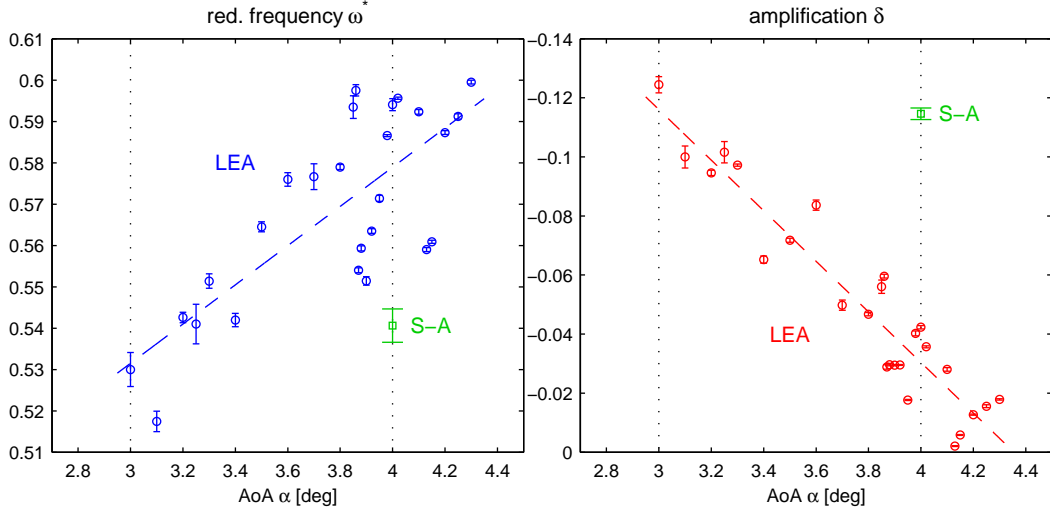
Figure 13: Reduced frequency and amplification rate identified from the lift impulse response for various steady flow fields. Error bars represent the standard deviation among the averaged windows during the curve fitting procedure. LEA and Spalart-Allmaras (S-A) turbulence models.

Fig. 13 shows the impulse response results for various angles of attack in the range $3° \leq \alpha \leq 4.3°$. Below 3° oscillations can be hardly noticed in the lift response and the identification of reasonable frequency and amplification values by time series curve fitting becomes increasingly difficult. As expected from the LCO and frequency response simulations in the preceding sections, frequency and amplification globally rise as α is increased. The frequency values at 3° and 4° are consistent with the peak locations in Fig. 6, while the ratio of the identified amplification rates reproduces the inverse ratio of the peak heights. Surprising is the broad local scattering of the identified shock buffet eigenvalue as α is changed by small amounts. Note the dramatic change of circa 10% in eigenfrequency as α is changed from 3.86° to 3.87°. In the light of such a local hypersensitivity to α the pitch excitation amplitude of $\Delta\alpha = 0.01°$ in the previous section might be questioned. The nonmonotonic evolution of the amplification rates has a remarkable consequence: Although not occuring here explicitly, in the vicinity of the stability boundary $\delta = 0$ amplification might become locally positive in a small α range – a tendency observed at 4.13°, where amplification suddenly jumps to −0.2% and later drops back to −1.8%.

Since special care is taken on accuracy and reproducibility of the eigenvalue identification from the lift signal, it can be excluded, that the observed eigenvalue scattering is an artefact of the curve fitting procedure or can be attributed to the randomized initial values. Recall from Fig. 5, that between $\alpha = 3°$ and 4° the shock-induced separation bubble merges with the trailing edge separation and thus the backflow topology and backflow dynamics is expected to change significantly over a small α interval. Nevertheless, model-inherent numerical uncertainties due to grid deficiencies or turbulence model issues are supposed to be the primary reason for the unexpected eigenvalue scattering. The sensitivity of the shock buffet eigenvalue to turbulence modeling is demonstrated exemplarily at $\alpha = 4°$, where the turbulence model is switched from LEA to Spalart-Allmaras for one simulation. Since the computed amplification values differ here by a factor of 3, a serious impact of turbulence modeling on the shock buffet onset estimation can be expected. This is already a consequence of the disparity of the mean flow fields (shock location, boundary layer structure, backflow topology etc.) predicted by different turbulence models.

12

From the results of the α-sweep simulation in section 3.1 a stable fixed-point solution (i.e. $\delta < 0$) up to $\alpha = 5.5°$ is expected. In contrast, the observed global damping trend in Fig. 13 seems to point to a stability limit near $\alpha \approx 4.5°$, which interestingly lies in the region of the least stable shock buffet LCO. An explanation for this apparent inconsistency can not yet be given.

4 CONCLUSIONS AND FURTHER WORK

After having identified the shock buffet onset of a supercritical airfoil at $Ma = 0.75$ by nonlinear time-accurate URANS simulations, various fixed-point stable flow fields below the shock buffet onset were excited by small perturbations within the same nonlinear solver. The small scale of the pertubation magnitudes caused the flow field to behave virtually like a linear system. Based on the frequency and impulse response of the flow to these small pertubations it was demonstrated, that the shock buffet phenomenon can be attributed to a natural resonance frequency of the steady transonic flow field in a linear sense.

The shock buffet resonance manifests itself in a $-180°$ phase reversal of the shock motion when the flow field is excited harmonically: Driving an airfoil in sinusoidal pitch motion yields inverse shock motion below the resonance frequency and regular shock motion above. A necessary condition for the low-frequency inverse shock motion, and thus for the shock buffet resonance, is shock-induced separation.

The flow field oscillates with the same frequency (and damping) for arbitrary small amplitudes. Hence, its oscillatory nature is seen to be an inherent property of the stable mean flow field around which the oscillation occurs. Nevertheless, the exact reason for the oscillatory disposition of the transonic flow field with separation remains to be explained, i.e. the feedback or "standing wave" mechanism in the shock buffet eigenmode is not yet understood. A consistent description of the feedback mechanism should not rely on the large scale effects observed after the degeneration of the damped linear resonance towards a nonlinear LCO, like cyclic vanishing and recurring of the shock or cyclic separation and reattachment of the boundary layer. An upcoming detailed study of the boundary layer dynamics, particularly of local integrated quantities like displacement and momentum thickness, is supposed to shed some light on this problem.

Since we expect the shock buffet onset problem to be treatable as a linearized stability problem, it would be of high interest to investigate the exact eigenvalues and eigenmodes of the flux Jacobian of recent linearized RANS solvers (e.g. [21]) in that context. Alternatively, a modal decomposition could be obtained by a principal component analysis in the time or frequency domain [22].

5 REFERENCES

[1] Lee, B. H. K. (2001). Self-sustained shock oscillations on airfoils at transonic speeds. *Progress in Aerospace Sciences*, 37(2), 147–196.

[2] Raveh, D. E. A Numerical Study of an Oscillating Airfoil in Transonic Flows With Large Shock Wave Oscillations. *AIAA-Paper 2008-1756*.

[3] Mcdevitt, J. B. and Okuno, A. F. (1985). Static and dynamic pressure measurements on a NACA 0012 airfoil in the Ames High Reynolds Number Fascility. Tech. rep., NASA-TP-2485.

[4] Jacquin, L., Molton, P., Deck, S., et al. (2005). An Experimental Study of Shock Oscillation over a Transonic Supercritical Profile. *AIAA-Paper 2005-4902*.

[5] Deck, S. (2005). Numerical simulation of transonic buffet over a supercritical airfoil. *AIAA Journal*, 43(7), 1556–1566.

[6] Šoda, A. (2007). *Numerical investigation of unsteady transonic shock/boundary-layer interaction for aeronautical applications.* PhD thesis, Deutsches Zentrum für Luft- und Raumfahrt, DLR-FB-2007-03.

[7] Finke, K. (1977). *Stoßschwingungen in schallnahen Strömungen.* Düsseldorf: Forschungsheft 580, VDI.

[8] Lee, B. H. K., Murty, H., and Jiang, H. (1994). Role of Kutta waves on oscillatory shock motion on an airfoil. *AIAA journal*, 32(4), 789–796.

[9] Gerhold, T., Friedrich, O., Evans, J., et al. (1997). Calculation of Complex Three-Dimensional Configurations Employing the DLR-TAU-Code. *AIAA-Paper 97-0167*.

[10] Schwamborn, D., Gerhold, T., and Heinrich, R. (2006). The DLR TAU-Code: Recent Applications in Research and Industry. In *Proc. of Europ. Conf. on Computational Fluid Dynamics ECCOMAS CFD*.

[11] Rung, T., Lübcke, H., Franke, M., et al. (1999). Assessment of Explicit Algebraic Stress Models in Transonic Flows. In *Proc. of 4th Symp. on Engineering Turbulence Modelling and Measurements, France.* Amsterdam: Elsevier, pp. 659–668.

[12] Nitzsche, J., Brouwers, K., Gardner, A. D., et al. (2008). Investigation of Unsteady Control Surface Aerodynamics on a 2D Supercritical Airfoil Model. In *Proc. of German Aerospace Congress DLRK2008*. DGLR.

[13] Spalart, P. R. and Allmaras, S. R. (1992). A one-equation turbulence model for aerodynamic flows. *AIAA-Paper 92-0439*, (1), 5–21.

[14] Rosemann, H. (1996). The Cryogenic Ludwieg-Tube at Göttingen. In *Special Course on Advances in Cryogenic Wind Tunnel Technology*, AGARD-R-812.

[15] Klioutchnikov, I. and Ballmann, J. (2006). DNS of Transitional Transonic Flow about a Supercritical BAC3-11 Airfoil using High-Order Shock Capturing Schemes. In *Direct and Large-Eddy Simulation VI*. Springer Netherlands, pp. 737–744.

[16] Crouch, J. D., Garbaruk, A., and Magidov, D. (2007). Predicting the onset of flow unsteadiness based on global instability. *Journal of Computational Physics*, 224(2), 924–940.

[17] Davis, S. S. and Malcolm, G. N. (1980). Transonic Shock-Wave/Boundary-Layer Interactions on an Oscillating Airfoil. *AIAA Journal*, 18(11), 1306–1312.

[18] Houwink, R. (1980). Some Remarks on Boundary Layer Effects on Unsteady Airloads. In *Proc. of 51st SMP meeting on "Boundary layer effects on unsteady airloads"*, AGARD-CP-296.

[19] Zwaan, R. J. (1985). Verification of calculation methods for unsteady airloads in the prediction of transonic flutter. *Journal of Aircraft*, 22(10), 833–839.

[20] den Boer, R. G. and Houwink, R. (1985). Analysis of transonic aerodynamic characteristics for a supercritical airfoil oscillating in heave, pitch and with oscillating flap. In *Proc. of 59th SMP meeting on "Transonic Unsteady Aerodynamics and its Aeroelastic Applications"*, AGARD-CP-374.

[21] Pechloff, A. and Laschka, B. (2006). Small Disturbance Navier-Stokes Method: Efficient Tool for Predicting Unsteady Air Loads. *Journal of Aircraft*, 43(1), 17–29.

[22] Dowell, E. H. and Hall, K. C. (2001). Modeling of Fluid-Structure Interaction. *Annual Review of Fluid Mechanics*, 33(1), 445–490.